



OPEN ACCESS

EDITED BY

R. Matthew Asmussen,
Pacific Northwest National Laboratory (DOE),
United States

REVIEWED BY

Zhaodong Liu,
Shandong Academy of Agricultural Sciences,
China

R. Matthew Asmussen,
Pacific Northwest National Laboratory (DOE),
United States

*CORRESPONDENCE

Vasileios A. Anagnostopoulos,
✉ vasileios.anagnos@ucf.edu

RECEIVED 12 November 2024

ACCEPTED 07 January 2025

PUBLISHED 10 February 2025

CITATION

Szlamkowicz IB, Ribeiro GB, Nguyen AT and
Anagnostopoulos VA (2025) The geochemical
control of birnessite on selenium fate and
transport at environmental concentrations.
Front. Environ. Chem. 6:1527112.
doi: 10.3389/fenvc.2025.1527112

COPYRIGHT

© 2025 Szlamkowicz, Ribeiro, Nguyen and
Anagnostopoulos. This is an open-access
article distributed under the terms of the
[Creative Commons Attribution License \(CC BY\)](https://creativecommons.org/licenses/by/4.0/).
The use, distribution or reproduction in other
forums is permitted, provided the original
author(s) and the copyright owner(s) are
credited and that the original publication in this
journal is cited, in accordance with accepted
academic practice. No use, distribution or
reproduction is permitted which does not
comply with these terms.

The geochemical control of birnessite on selenium fate and transport at environmental concentrations

Ilana B. Szlamkowicz, Giovanna B. Ribeiro, Anna T. Nguyen and
Vasileios A. Anagnostopoulos*

Department of Chemistry, University of Central Florida, Orlando, FL, United States

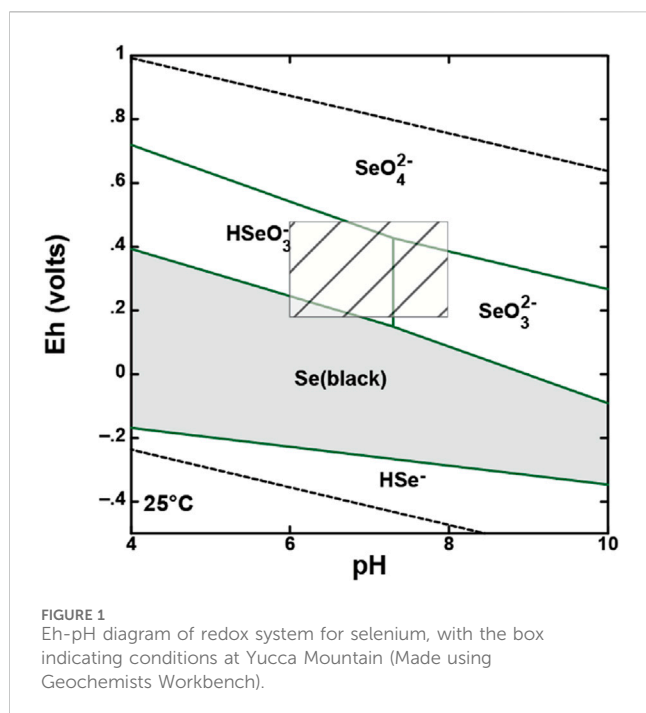
This study investigated the geochemical controls on selenium mobility by two forms of birnessite mineral, focusing on the influence of pH, concentration, and the presence of cations. The research aimed to understand the dominant reaction mechanism (redox vs. sorption) under environmentally relevant selenium concentrations. Experiments were conducted to study the interaction of selenium with the birnessite minerals under varying conditions. The results demonstrated a significant shift in the dominant reaction mechanism from slow redox reactions observed at artificially elevated selenium concentrations to fast sorption processes at environmentally relevant concentrations, with second order rates increasing from 7.63×10^{-7} to $0.0224 \text{ L mol}^{-1} \text{ h}^{-1}$, respectively. This finding highlights the crucial role of selenium concentration in determining its interaction with birnessite minerals and emphasizes the importance of conducting research under realistic conditions to accurately predict selenium mobility and develop effective remediation strategies.

KEYWORDS

manganese oxide, birnessite, selenium, selenite, sorption, oxidation

Introduction

Deep geological repositories (DGR) are used to contain and isolate spent nuclear fuel which contains many radionuclides. One such DGR is Yucca Mountain in Nevada, which had been proposed as a storage facility for spent nuclear fuel and high-level radioactive waste. The contained waste would also contain the fission by-products produced within the storage tanks. Selenium-79 is produced as a fission product from uranium-235, and has a half-life of 6.5×10^4 years (Martinez et al., 2006; Brennetot et al., 2008). Selenium has five naturally occurring stable isotopes (Se-74, Se-76, Se-77, Se-78, Se-80) and twenty-four radioactive isotopes (Preedy, 2015). In nuclear waste repositories, immobilization methods are utilized to reduce Se-79 concentrations in the nearfield of the repository (Aurelio et al., 2010). Another method of selenium release into the environment is the point source contamination of local ground waters, from sources such as coal-fired electrical generating stations sites (Aurelio et al., 2010). These commercial coal-burning plants release selenium, one of the two most volatile and potentially hazardous elements from this process, which is released through fugitive emissions, fly ash, and bottom ash (Huggins et al., 2007). This release of coal fly ash presents an avenue for selenium to leach out from coal-burning electrical generating sites into the environment (Wang et al., 2009).



Selenium also plays an important role in cellular processes as a key component in selenoproteins and selenoenzymes, which are crucial to biological functions such as the transport and storage of selenium (Sun et al., 2014). While a deficiency in selenium intake can cause diseases such as Keshan (a juvenile, multifocal myocarditis) or mulberry heart disease, an excess intake of selenium has been seen to induce cancer (Reich and Hondal, 2016; World Health Organization, 2022). Additionally, proper dosages of selenium has been seen to influence the prevention of certain cancers (Sun et al., 2014). Selenium can be considered both a toxin and an essential nutrient to bacteria and animal species, though it is naturally present at low concentrations (most being lower than 10 $\mu\text{g/L}$, except in certain seleniferous areas) (Reich and Hondal, 2016; World Health Organization, 2022; Sharma et al., 2019). The World Health Organization has established a toxic limit for selenium in human adults of 400 $\mu\text{g/day}$ and the Environmental Protection Agency has set the drinking water maximum contamination level (MCL) at 50 mg/L , indicating that exposure should be monitored (Reich and Hondal, 2016; Gonzalez et al., 2011). Though the natural environmental concentration and the daily toxic limit for selenium are both at trace level, there has been a deficit of studies undertaken at this concentration.

Previous studies have been conducted using concentrations magnitudes higher than these realistic levels, ranging from 3 to 500 μM (Martinez et al., 2006; Dwivedi et al., 2022; Scott and Morgan, 1996). The use of artificially elevated concentrations has been historically attributed to instruments having higher limits of detections. It has been observed previously that the starting concentration of an analyte significantly impacts a reaction, influencing the development of analytical techniques with lower detection limits (Szlankowicz et al., 2023). Here, a tandem ion chromatography-inductively coupled plasma-mass spectroscopy (IC-ICP-MS) method was developed to allow for the analysis of selenium at environmentally realistic trace level concentrations.

There are multiple oxidation states that selenium can be found under: -2 , 0 , $+2$, $+4$, and $+6$ (Preedy, 2015). Under environmental conditions, selenium is predominantly found as a stable inorganic oxyanion (Scott and Morgan, 1996). These selenium oxyanion species are SeO_3^{2-} and SeO_4^{2-} , selenite [Se(IV)] and selenate [Se(VI)], respectively. Under very strong oxidizing conditions, SeO_4^- is the predominant species, while at mild oxidizing conditions, SeO_3^- is most present (Figure 1) (Sharma et al., 2019). It is important to understand the speciation of selenium, as selenite is more toxic towards eukaryotes and prokaryotes than selenate is (Sun et al., 2014). Additionally, the oxidation state of the oxyanion alters the affinity of the compound towards metal oxide surfaces, as well as the complexing mechanism (Scott and Morgan, 1996). In soil, there are various minerals that regulate the speciation, as well as the fate and transport, of selenium, one such of this being manganese oxide minerals (Dwivedi et al., 2022; Scott and Morgan, 1996; Scott, 1991).

Manganese oxides are an abundant group of minerals that can be found in soils. Their concentrations in soils range from less than 7–9,000 mg kg^{-1} , and they make up about 0.1% of Earth's crust (Hooda, 2010; Post, 1999). The presence of manganese oxide minerals has been observed in DGR's like Yucca Mountain, controlling the Eh of the system in the 0.2–0.5 V range for pH 6–8 (Caporuscio and Vaniman, 1985). In the case of Yucca Mountain, manganese oxides are concentrated along fractures rather than in the bulk rock, which may further influence geochemical contributions. Manganese oxides are made up of MnO_6 octahedra, where the structure is dependent on whether the octahedra shares corners and/or edges with each other, and can have corner-connected subunits forming tunnels or edge-sharing stacked layered structures (Post, 1999; Remucal and Ginder-Vogel, 2014). These various manganese oxide minerals have a high redox potential, exerting geochemical control over almost any metal and metalloid species in the environment (Post, 1999; Ukrainczyk and McBride, 1992; Haynes, 2016; Wang and Giammar, 2015). Besides a high oxidative capacity, manganese oxides also exhibit high sorption capabilities, due to poor crystallinity, high specific surface area, and highly reactive vacancy sites (Wang and Giammar, 2015; Fischel et al., 2015).

Birnessite [$(\text{Mn(III)/Mn(IV)})_2\text{O}_4$] is the most common manganese oxide, due to its production from Mn(II) oxidizing bacteria during manganese cycling (Post, 1999). It exhibits a layered structure, possessing both oxidation-reduction and cation-exchange capabilities (Villalobos et al., 2003). This is possible because the vacancies in between the layers cause birnessite to have a net negative charge, with the charge being compensated in the interlayer region by hydrated metal ions (Arias et al., 2013; Becerra et al., 2011). For the birnessite family of minerals, synthesis conditions are seen to affect the ionic conductivity of the different birnessites on account of alterations in the minerals (Arias et al., 2019).

Two forms of birnessite minerals are used here: acid birnessite and “c-disordered” H^+ birnessite. Acid birnessite has a hexagonal layer structure, with a relatively high stacking order between its layers and has potassium as the predominant interlayer cation (Fischel et al., 2015; Wang et al., 2016; Wang et al., 2018). The “c-disordered” H^+ birnessite is a manganese oxide with hexagonal symmetry, corner sharing octahedra, and a high density of layer vacancies allowing for high sorption capacity (Friedl et al., 1997). Additionally, there is a greater amount of Mn(III) spaced irregularly along the *b*-axis in “c-disordered” H^+ birnessite, pushing into the

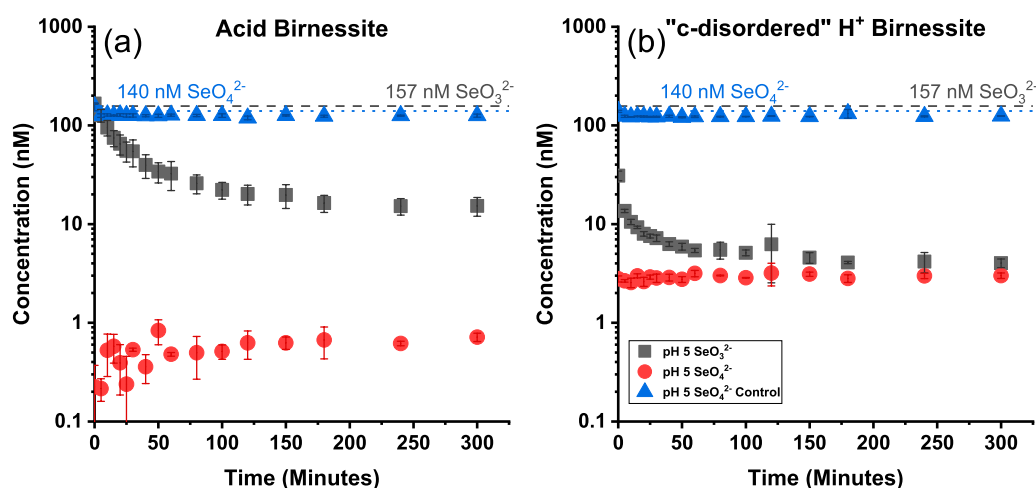


FIGURE 2
Concentration of selenium for Acid Birnessite (A) and "c-disordered" H⁺ Birnessite (B) as a function of time for varying birnessite minerals under realistic concentrations of SeO₃²⁻. Blue dotted line indicates starting concentration of SeO₄²⁻ control. Grey dashed line indicates starting concentration of SeO₃²⁻.

c-direction (the interlayer region) of the mineral (Manceau et al., 2002).

Manganese oxide minerals, especially birnessites, have been previously observed to react extensively with a variety of anionic contaminants. These interactions encompass both sorptive and reduction-oxidation processes with selenium (Gonzalez et al., 2011; Dwivedi et al., 2022; Scott and Morgan, 1996). However, these studies don't account for different forms of birnessite minerals or the use of environmentally relevant concentrations of the contaminants. Different birnessite minerals have significantly different physical properties, which play key roles in reactivity. Additionally, the concentration of reactants play a key role in the reactivity of selenium.

In this study, we investigate the effect of initial concentration on the reactivity of selenium, using two different birnessite minerals at environmentally relevant pH values. The sorption of common cations on to the birnessite minerals was also investigated, to determine the resulting impact on the oxidation of selenium. The resulting speciation of selenium under realistic concentrations illustrates the controls that birnessite minerals exert on the fate and transport of this contaminant. The concentration dependent studies were conducted to compare the redox chemistry of selenium under artificially elevated concentrations (attributed to instrumentation limitations) to that of environmentally realistic concentrations. By using realistic concentrations, proper remediation strategies can be devised for contaminants in the environment.

Experimental

Mineral synthesis

Acid birnessite was synthesized using the acid reduction method from McKenzie (1971) A 42 mL solution of 10 M HCl (certified ACS

TABLE 1 Percent oxidation of SeO₃²⁻ at realistic concentrations for both acid and "c-disordered" H⁺ birnessite as a function of pH from experimental data.

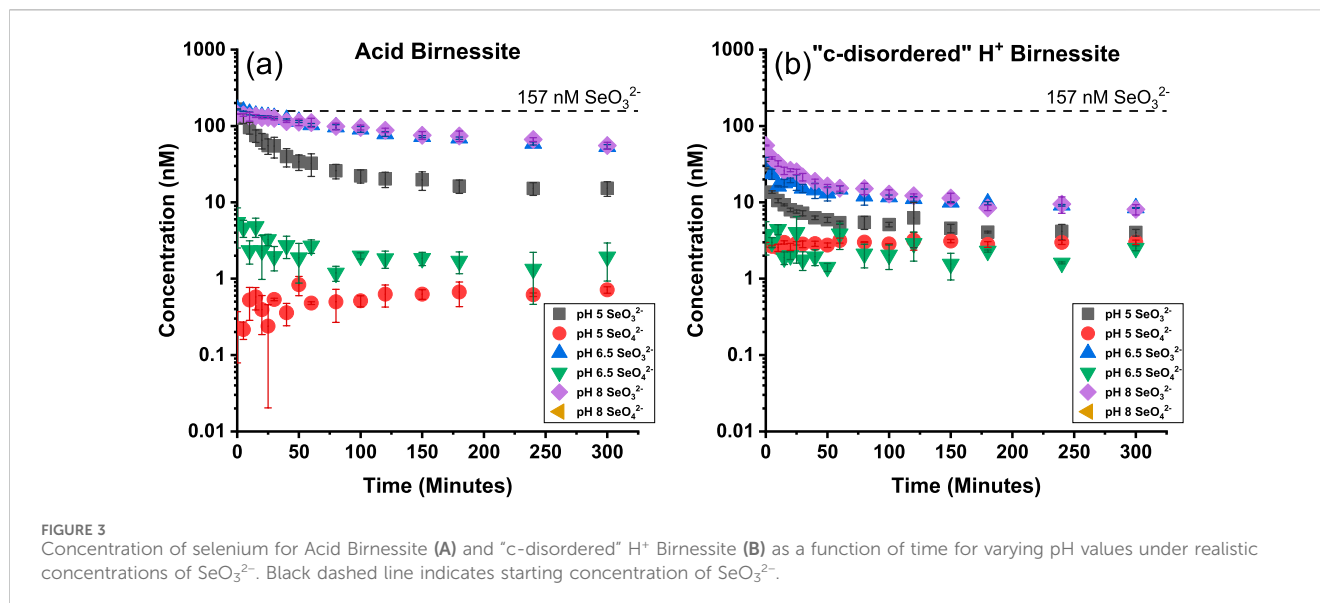
pH value	Acid birnessite	"c-disordered" H ⁺ birnessite
5	90% ± 2	97% ± 0.2
6.5	66% ± 2	94% ± 0.04
8	64% ± 4	95% ± 0.8

Plus grade, Fisher Chemical) was added dropwise to a vigorously boiling 0.58 L solution of 0.40 M KMnO₄ (Beantown Chemical, 99%) in ultrapure water (with a resistivity of 18.2 MΩ.cm). After the addition of the acid, the solution was boiled for an additional 10 min and cooled to room temperature. Using vacuum filtration with filter paper (Fisher Brand, P2 fine porosity glass fiber filter paper), the precipitate was isolated and washed with ultrapure water until the pH was 6. Then the precipitate was dried for 72 h in a 60°C oven.

The "c-disordered" H⁺ birnessite was synthesized using the redox methods from Villalobos et al. (2003) A 160 mL solution of 0.20 M KMnO₄ was stirred, while a solution of 180 mL of 0.51 M NaOH (Alfa Aesar, 98%) was slowly added. Next, a 160 mL solution of 0.58 M MnCl₂ (Acros Organics, 99%) was slowly added to the mixture before settling for 4 h. Using the triclinic sodium-birnessite method, the suspension was washed with a solution of 1.0 M NaCl (Fisher Bioreagents, 99.5%) and ultrapure water. Then using NaOH, the pH was adjusted to 8. The precipitate was then dried for 72 h in a 50°C oven.

Batch experiments

In order to monitor and quantify the kinetics of the oxidation of SeO₃²⁻ to SeO₄²⁻, batch experiments were conducted using the different birnessites as a function of concentration level at



varying pH in 50 mL centrifuge tubes. Each mineral was suspended in ultrapure water and adjusted to the desired pH before being spiked with a stock solution of SeO₃²⁻ (as NaSeO₃, VWR, high purity grade). The pH of the solution was periodically checked and adjusted using HCl or NaOH. At specific time points, the samples were centrifuged for 10 min at 5,000 rpm (ThermoScientific, Sorvall ST16 Centrifuge). For analysis, an aliquot of the supernatant was taken to be analyzed using tandem ion chromatography–inductively coupled plasma–mass spectroscopy (IC-ICP-MS). Sorption control experiments were performed under identical conditions, but spiked with SeO₄²⁻ (as NaSeO₄, ThermoFisher Scientific, 99.8+% purity) instead of SeO₃²⁻. These experiments were conducted to determine if the mineral will retain the analyte and cause an underestimation of the SeO₄²⁻ concentration. Additional control experiments were conducted to determine the volatility of the selenium species under the investigated conditions, where SeO₃²⁻ and SeO₄²⁻ were spiked into solutions of ultrapure water at the desired pH values.

Selenium speciation and elemental analysis

The two selenium species were analyzed using tandem IC-ICP-MS, with the individual instrument conditions having been described in Szlamkowicz et al. (2022). This tandem method allows for the simultaneous speciation and quantification of selenium at environmentally realistic concentrations (nM range). This occurs through the IC separating the different species of selenium using a selective ion exchange column, the effluent of which is fed into the ICP-MS through a capillary line. Since the ICP-MS has much lower limits of detection than the IC does on its own, it was used as a detector in place of the one within the IC. Thus, tandem IC-ICP-MS combines the separatory capabilities of IC with the low limits of detection of an ICP-MS, all in a single analytical step.

Solid characterization

The two birnessite minerals were characterized using X-ray diffraction (XRD, Empyrean, PANalytical), with analysis parameters having been previously described in Stanberry et al. (2021a) and Stanberry et al. (2021b). Additionally, the manganese average oxidation state (AOS), specific surface area, and pH where the surface of the mineral has a net neutral charge (pH_{pzc}) was performed, with the results having been described previously in Szlamkowicz et al. (2023).

Results and discussion

Impact of birnessite mineral

Two different forms of the oxidizing agent, birnessite, are initially investigated to determine its influence on the oxidation of selenium under environmental conditions. The two forms of birnessite used are acid birnessite and "c-disordered" H⁺ birnessite, whose main differences in mineral structure has been established previously by Szlamkowicz et al., with the X-ray diffraction (XRD) patterns seen in Supplementary Figure S1 (Szlamkowicz et al., 2023). These two minerals exhibit various degrees of reactivity towards selenite (SeO₃²⁻), as seen below in Figure 2. The concentration of SeO₃²⁻ in solution decreases more rapidly and extensively with the "c-disordered" H⁺ birnessite as compared to the acid birnessite. The rapid disappearance of Se in the aqueous phase is attributed to the fast and strong adsorption of SeO₃²⁻ onto the active sites along the surface of the mineral through strong inner-sphere complexes (Dwivedi et al., 2022). The disappearance of SeO₃²⁻ in solution with the "c-disordered" H⁺ birnessite was quite rapid leading to only the data from acid birnessite being used when trying to determine the reaction order for these experiments. It was determined that the reaction between SeO₃²⁻ and acid birnessite follows a second order reaction, as seen in Supplementary Figure S2. It was determined that

TABLE 2 Summary of average concentrations and standard deviations of sorbed SeO_3^{2-} onto cation sorbed and plain birnessite minerals, as well as the corresponding p values illustrating the results not being statistically different.

Acid birnessite SeO_3^{2-} Concentrations (nM)				"c-disordered" H^+ birnessite SeO_3^{2-} Concentrations (nM)			
Plain	Ca^{2+}	Mn^{2+}	Na^+	Plain	Ca^{2+}	Mn^{2+}	Na^+
128 ± 10	103 ± 12 ($p = 0.053$)	136 ± 12 ($p = 0.38$)	113 ± 5 ($p = 0.079$)	116 ± 8	99 ± 10 ($p = 0.078$)	112 ± 8 ($p = 0.55$)	108 ± 2 ($p = 0.15$)

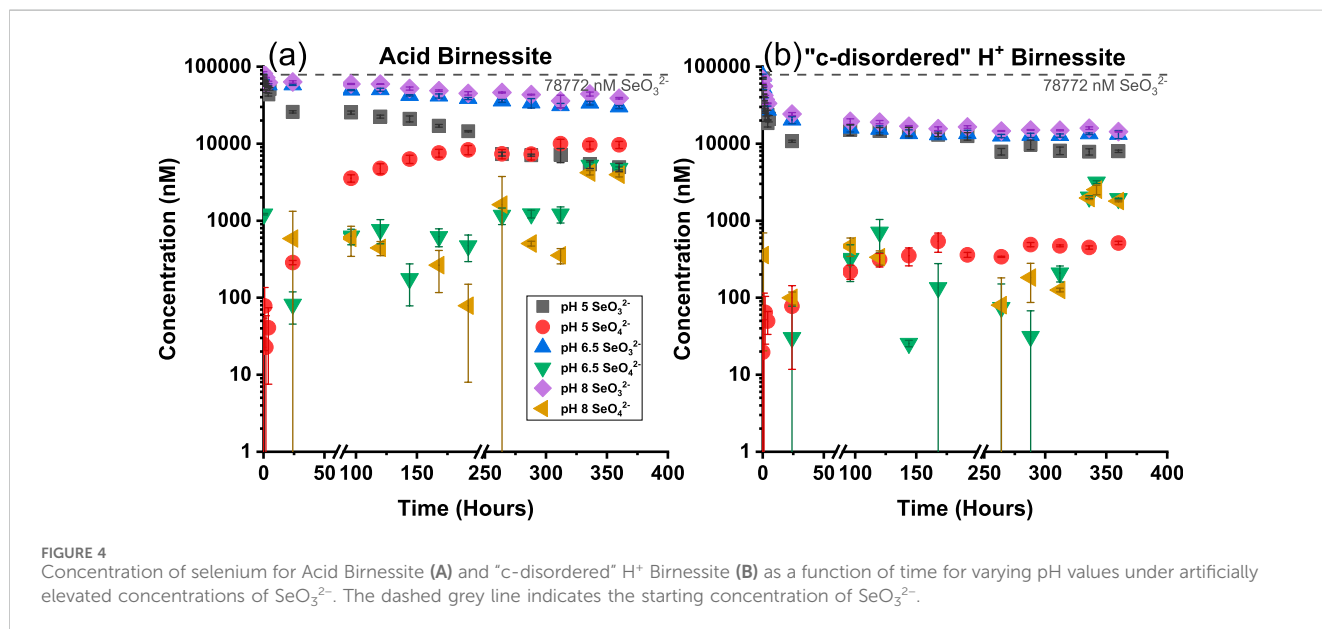


TABLE 3 Percent oxidation of selenium at artificially elevated concentrations for both acid and "c-disordered" H^+ birnessite as a function of pH.

pH value	Acid birnessite	"c-disordered" H^+ birnessite
5	$94\% \pm 0.7$	$90\% \pm 0.4$
6.5	$62\% \pm 2$	$84\% \pm 1$
8	$51\% \pm 2$	$82\% \pm 0.2$

the reaction rate constant was $3.73 \times 10^{-4} \text{ M}^{-1} \text{ min}^{-1}$. This follows the second order reaction observed in a previous study, where the sorption and oxidation of SeO_3^{2-} was studied using a birnessite mineral in stirred flow reactors (Balistrieri and Chao, 1990).

In the case of both birnessite minerals at pH 5, there is a significant disappearance of SeO_3^{2-} from the solution and no release of selenate (SeO_4^{2-}) into the aqueous phase. This is attributed to the lower pH of the system exhibiting a weaker electrostatic repulsion between SeO_3^{2-} and the surface of the mineral, which results in a greater extent of sorption (Balistrieri and Chao, 1990). This is attributed to the selenite in the system forming inner-sphere complexes, while selenate forms outer-sphere complexes with MnO_2 minerals (Li et al., 2021). Electrostatic interactions cause selenite to form outer-sphere complexes, while inner-sphere complexes require more than purely Coulombic forces (Balistrieri and Chao, 1990). Control samples of SeO_4^{2-} were

prepared, to determine if there is a sorption mechanism of SeO_4^{2-} in the system, which would cause an underestimation of the mass balance of selenium. However, the sorption controls of SeO_4^{2-} indicate that the minerals are capable of negligible levels of sorption (Figure 2). This indicates that the disappearance of selenium from the aqueous phase is only a result of the sorption of SeO_3^{2-} , and not from oxidation. This is due to SeO_3^{2-} having a much stronger adsorption to metal oxide surfaces through the formation of strong inner-sphere complexes (Dwivedi et al., 2022). Conversely, SeO_4^{2-} adsorbs to metal oxide surfaces through weaker outer-sphere complexes (Dwivedi et al., 2022). This follows XPS data from Li et al. where the post reaction solids only exhibited the reduced form of selenium, SeO_3^{2-} (Balistrieri and Chao, 1990).

Effect of solution pH

The percent of SeO_3^{2-} oxidized under the varying pH values for both minerals has been summarized below in Table 1. As the pH increased, acid birnessite experienced a decrease in the extent of SeO_3^{2-} sorption, from $90\% \pm 2$ at pH 5– $64\% \pm 4$ at pH 8. However, the "c-disordered" H^+ birnessite was not impacted by the increasing pH (Figure 3). This disparity is attributed to the "c-disordered" H^+ birnessite having a consistent net surface charge throughout the different investigated pH values. The reason the "c-disordered" H^+ birnessite was less affected by the increase in pH of

the system is due to it having a lower pH_{pzc} for the vacancy sites than acid birnessite, <3 and 3.5–4.0, respectively (Szlankowicz et al., 2023; Arias et al., 2019). Acid birnessite has a pH_{pzc} that is closer to pH 5, causing the vacancy sites to have more positive sites amidst the negative sites along the mineral surface. On the other hand, the surface of “c-disordered” H^+ birnessite has a mostly negative charge, with few residually positive charged vacancy sites. The mostly negative charge is due to the pH of the system being above the pH_{pzc} of “c-disordered” H^+ birnessite. Some residual positive vacancy sites remain on the mineral since the pH of the system is close to the pH_{pzc} values. The residual positive active sites will have a greater electrostatic attraction to SeO_3^{2-} at pH 5, which will decrease as the pH increases to 8 and the sites become negatively charged. With this, “c-disordered” H^+ birnessite was able to sorb $97\% \pm 0.2$ at pH 5, and $95\% \pm 0.8$ at pH 8.

The greater extent of disappearance of SeO_3^{2-} in the experiments using the “c-disordered” H^+ birnessite can be attributed to it having a higher specific surface area ($111 \text{ m}^2\text{g}^{-1}$) than acid birnessite ($35 \text{ m}^2\text{g}^{-1}$) (Szlankowicz et al., 2023). A greater specific surface area indicates a larger number of surface sites for SeO_3^{2-} sorption.

Cation sorption onto minerals

Common environmental cations were sorbed onto the two birnessite minerals, to determine if there is an effect of surface passivation. If the active sites on the birnessite mineral were preoccupied by the presence of the sorbed cations, there is the possibility of a decrease in the sorption of selenium in the system. The cations investigated were Ca^{2+} (CaCl_2 , Fisher Bioreagents), Mn^{2+} (MnCl_2 , 99+%, Thermo Scientific), and Na^+ (NaCl , Certified ACS, Fisher Chemical). To prepare the sorbed birnessites for use in selenium experiments, the minerals were suspended in a 50 mg L^{-1} solution of each cation. These mineral suspensions were allowed to spin for 3 weeks, prior to separating the supernatant and analyzing using ICP-MS. The minerals were rinsed using 10 mL of ultra-pure water, before sequestering the supernatant for analysis, to monitor for any cation loss during the washing phase.

Significant extents of sorption was observed for all cations on both birnessite minerals, as summarized in Supplementary Table S1. However, there was no statistical difference in the sorption of SeO_3^{2-} between the cation sorbed and plain birnessite minerals, as summarized in Table 2 and in Supplementary Figures S3, S4. This is attributed to there being two different active sites on the surface of birnessite minerals, each with a different localized charge. Having a positively charged edge site allows SeO_3^{2-} to readily sorb. On the other hand, the Ca^{2+} , Mn^{2+} , and Na^+ are sorbed onto the negatively charged vacancy sites of the mineral.

Artificially elevated concentrations

Artificially elevated concentrations of SeO_3^{2-} were also used to investigate the concentration dependency of SeO_3^{2-} when reacted with both acid and “c-disordered” H^+ birnessites. Similar to previous experiments conducted at realistic concentrations of SeO_3^{2-} , it was seen that as the pH increased, the extent of sorption decreased with acid birnessite while remaining unchanged with the “c-disordered”

H^+ birnessite (Figure 4). The percent of SeO_3^{2-} sorbed under the varying pH values for both minerals at elevated concentrations has been summarized below in Table 3. Even throughout the experiments with an elevated initial SeO_3^{2-} concentration, there was minimal observed oxidation to SeO_4^{2-} . The only exception to this trend was with acid birnessite at pH 5, where there was a $12\% \pm 1$ formation and release of SeO_4^{2-} during the reaction.

However, it is important to note that the formation of SeO_4^{2-} does not begin to appear until a hundred hours into the experiment at artificially elevated concentrations (Figure 4), depending on both the mineral and the pH. Conversely, the experiments using environmentally realistic concentrations (Figure 3) reach equilibrium within 5 h. This illustrates the elevated concentration reaction being a slow sorptive and oxidative process. This can be further seen in Supplementary Figures S2, S5, where the SeO_3^{2-} reaction rates are depicted for the disappearance of SeO_3^{2-} . In these figures, it is observed that the rate of sorption is much slower when using artificially elevated concentrations of SeO_3^{2-} . This difference of time frame and reactivity is important to understand when devising remediation methods for selenium contamination in the environment.

Conclusion

This study investigated selenium reactivity under environmentally relevant conditions, focusing on the influence of birnessite minerals, pH, and low SeO_3^{2-} concentrations. Our results demonstrate a significant divergence from previous studies conducted at artificially high selenium levels, highlighting the critical importance of using environmentally realistic concentrations to accurately predict selenium behavior. We found that sorption, rather than redox reactions, predominates in the interaction between SeO_3^{2-} and the two birnessite minerals studied. This research underscores the need to consider the specific mineralogy of birnessite and its impact on selenium mobility when developing effective remediation strategies.

Data availability statement

The raw data supporting the conclusions of this article will be made available by the authors, without undue reservation.

Author contributions

IS: Data curation, Formal Analysis, Investigation, Validation, Visualization, Writing—original draft, Writing—review and editing. GR: Investigation, Writing—original draft. AN: Investigation, Writing—original draft. VA: Conceptualization, Funding acquisition, Project administration, Resources, Supervision, Writing—review and editing.

Funding

The author(s) declare that financial support was received for the research, authorship, and/or publication of this article. This

manuscript was prepared under awards 31310019M0010 and 31310023M0017 from the Nuclear Regulatory Commission.

Acknowledgments

The statements, findings, conclusions, and recommendations are those of the author(s) and do not necessarily reflect the view of the US Nuclear Regulatory Commission. The authors are grateful for the assistance of the scientists of the Materials Characterization Facility, AMPAC at the University of Central Florida during XRD data collection.

Conflict of interest

The authors declare that the research was conducted in the absence of any commercial or financial relationships that could be construed as a potential conflict of interest.

References

- Arias, N., Dávila, M., and Giraldo, O. (2013). Electrical behavior of an octahedral layered OL-1-type manganese oxide material. *Ionics* 19 (2), 201–214. doi:10.1007/s11581-012-0725-9
- Arias, N. P., Becerra, M. E., and Giraldo, O. (2019). Structural and electrical studies for birnessite-type materials synthesized by solid-state reactions. *Nanomaterials* 9 (8), 1156. doi:10.3390/nano9081156
- Aurelio, G., Fernández-Martínez, A., Cuello, G. J., Román-Ross, G., Alliot, I., and Charlet, L. (2010). Structural study of selenium(IV) substitutions in calcite. *Chem. Geol.* 270 (1), 249–256. doi:10.1016/j.chemgeo.2009.12.004
- Balistreri, L. S., and Chao, T. (1990). Adsorption of selenium by amorphous iron oxyhydroxide and manganese dioxide. *Geochimica et Cosmochimica Acta* 54 (3), 739–751. doi:10.1016/0016-7037(90)90369-v
- Becerra, M., Arias, N., Giraldo, O., Suárez, F. L., Gómez, M. I., and López, A. B. (2011). Soot combustion manganese catalysts prepared by thermal decomposition of KMnO₄. *Appl. Catal. B Environ.* 102 (1–2), 260–266. doi:10.1016/j.apcatb.2010.12.006
- Brennetot, R., Pierry, L., Atamyan, T., Favre, G., and Vailhen, D. (2008). Optimisation of the operating conditions of a quadrupole ICP-MS with hexapole collision/reaction cell for the analysis of selenium-79 in spent nuclear fuel using experimental designs. *J. Anal. Atomic Spectrom.* 23 (10), 1350–1358. doi:10.1039/b802820f
- Caporuscio, F. A., and Vaniman, D. (1985). *Iron and manganese in oxide minerals and in glasses: preliminary consideration of Eh buffering potential at Yucca Mountain, Nevada*. Los Alamos, NM (United States): Los Alamos National Lab.LANL.
- Dwivedi, P., Schilling, K., Wasserman, N., Johnson, T. M., and Pallud, C. (2022). Oxidation of dissolved tetravalent selenium by birnessite: Se isotope fractionation and the effects of pH and birnessite structure. *Front. Earth Sci.* 10, 909900. doi:10.3389/feart.2022.909900
- Fischel, J. S., Fischel, M. H., and Sparks, D. L. (2015). “Advances in understanding reactivity of manganese oxides with arsenic and chromium in environmental systems,” in *Advances in the environmental biogeochemistry of manganese oxides* (American Chemical Society), 1197, 1–27. doi:10.1021/bk-2015-1197.ch001
- Friedl, G., Wehrli, B., and Manceau, A. (1997). Solid phases in the cycling of manganese in eutrophic lakes: new insights from EXAFS spectroscopy. *Geochimica Cosmochimica Acta* 61 (2), 275–290. doi:10.1016/s0016-7037(96)00316-x
- Gonzalez, C. M., Hernandez, J., Parsons, J. G., and Gardea-Torresdey, J. L. (2011). Adsorption of selenite and selenate by a high- and low-pressure aged manganese oxide nanomaterial. *Instrum. Sci. Technol.* 39 (1), 1–19. doi:10.1080/10739149.2010.537721
- Haynes, W. M. (2016). *CRC handbook of chemistry and physics*. Boca Raton, FL, United States: CRC Press.
- Hooda, P. S. (2010). “Trace elements in soils,” 618. Wiley Online Library.
- Huggins, F. E., Senior, C. L., Chu, P., Ladwig, K., and Huffman, G. P. (2007). Selenium and arsenic speciation in fly ash from full-scale coal-burning utility plants. *Environ. Sci. and Technol.* 41 (9), 3284–3289. doi:10.1021/es062069y
- Li, Z., Yuan, Y., Ma, L., Zhang, Y., Jiang, H., He, J., et al. (2021). Simultaneous kinetics of selenite oxidation and sorption on δ-MnO₂ in stirred-flow reactors. *Inter. J. Environ. Res. Public Health* 18 (6), 2902.
- Manceau, A., Lanson, B., and Drits, V. A. (2002). Structure of heavy metal sorbed birnessite. Part III: results from powder and polarized extended X-ray absorption fine structure spectroscopy. *Geochimica Cosmochimica Acta* 66 (15), 2639–2663. doi:10.1016/s0016-7037(02)00869-4
- Martinez, M., Giménez, J., De Pablo, J., Rovira, M., and Duro, L. (2006). Sorption of selenium (IV) and selenium (VI) onto magnetite. *Appl. Surf. Sci.* 252 (10), 3767–3773. doi:10.1016/j.apsusc.2005.05.067
- McKenzie, R. M. (1971). The synthesis of birnessite, cryptomelane, and some other oxides and hydroxides of manganese. *Mineral. Mag.* 38 (296), 493–502. doi:10.1180/minmag.1971.038.296.12
- Post, J. E. (1999). Manganese oxide minerals: crystal structures and economic and environmental significance. *Proc. Natl. Acad. Sci.* 96 (7), 3447–3454. doi:10.1073/pnas.96.7.3447
- Preedy, V. R. (2015). *Selenium: chemistry, analysis, function and effects*. Cambridge, United Kingdom: Royal Society of Chemistry.
- Reich, H. J., and Hondal, R. J. (2016). Why nature chose selenium. *ACS Chem. Biol.* 11 (4), 821–841. doi:10.1021/acschembio.6b00031
- Remucal, C. K., and Ginder-Vogel, M. (2014). A critical review of the reactivity of manganese oxides with organic contaminants. *Environ. Sci. Process. and Impacts* 16 (6), 1247–1266. doi:10.1039/c3em00703k
- Scott, M. J. (1991). *Kinetics of adsorption and redox processes on iron and manganese oxides: reactions of arsenic (III) and selenium (IV) at goethite and birnessite surfaces*. Pasadena, CA, United States: California Institute of Technology.
- Scott, M. J., and Morgan, J. J. (1996). Reactions at oxide surfaces. 2. Oxidation of Se (IV) by synthetic birnessite. *Environ. Sci. and Technol.* 30 (6), 1990–1996. doi:10.1021/es950741d
- Sharma, V. K., Sohn, M., and McDonald, T. J. (2019). Remediation of selenium in water: a review. *Adv. water Purif. Tech.*, 203–218. doi:10.1016/b978-0-12-814790-0.00008-9
- Stanberry, J., Szlamkowicz, I., Magno, D., Shultz, L., and Anagnostopoulos, V. (2021a). Oxidative dissolution of TcO₂ by Mn (III) minerals under anaerobic conditions: implications on technetium-99 remediation. *Appl. Geochem.* 127, 104858. doi:10.1016/j.apgeochem.2020.104858
- Stanberry, J., Szlamkowicz, I., Purdy, L. R., and Anagnostopoulos, V. (2021b). TcO₂ oxidative dissolution by birnessite under anaerobic conditions: a solid-solid redox reaction impacting the environmental mobility of Tc-99. *Environ. Sci. Process. and Impacts* 23 (6), 844–854. doi:10.1039/d1em00011j
- Sun, H.-J., Rathinasabapathi, B., Wu, B., Luo, J., Pu, L.-P., and Ma, L. Q. (2014). Arsenic and selenium toxicity and their interactive effects in humans. *Environ. Int.* 69, 148–158. doi:10.1016/j.envint.2014.04.019

Generative AI statement

The author(s) declare that no Generative AI was used in the creation of this manuscript.

Publisher's note

All claims expressed in this article are solely those of the authors and do not necessarily represent those of their affiliated organizations, or those of the publisher, the editors and the reviewers. Any product that may be evaluated in this article, or claim that may be made by its manufacturer, is not guaranteed or endorsed by the publisher.

Supplementary material

The Supplementary Material for this article can be found online at: <https://www.frontiersin.org/articles/10.3389/fenvc.2025.1527112/full#supplementary-material>

- Szlankowicz, I. B., Fentress, A. J., Longen, L. F., Stanberry, J. S., and Anagnostopoulos, V. A. (2022). Transformations and speciation of iodine in the environment as a result of oxidation by manganese minerals. *ACS Earth Space Chem.* 6 (8), 1948–1956. doi:10.1021/acsearthspacechem.1c00372
- Szlankowicz, I. B., Roman, L. M. C., Hunley, L. M., Carroll, A. B., Pereira, B. B., and Anagnostopoulos, V. A. (2023). Structural contributions of different manganese oxide minerals on the redox transformations and proliferation of iodine. *Chemosphere* 339, 139631. doi:10.1016/j.chemosphere.2023.139631
- Ukrainczyk, L., and McBride, M. B. (1992). Oxidation of phenol in acidic aqueous suspensions of manganese oxides. *Clays Clay Min.* 40 (2), 157–166. doi:10.1346/ccmn.1992.0400204
- Villalobos, M., Toner, B., Bargar, J., and Sposito, G. (2003). Characterization of the manganese oxide produced by *pseudomonas putida* strain MnB1. *Geochimica Cosmochimica Acta* 67 (14), 2649–2662. doi:10.1016/s0016-7037(03)00217-5
- Wang, Q., Liao, X., Xu, W., Ren, Y., Livi, K. J., and Zhu, M. (2016). Synthesis of birnessite in the presence of phosphate, silicate, or sulfate. *Inorg. Chem.* 55 (20), 10248–10258. doi:10.1021/acs.inorgchem.6b01465
- Wang, Q., Yang, P., and Zhu, M. (2018). Structural transformation of birnessite by fulvic acid under anoxic conditions. *Environ. Sci. and Technol.* 52 (4), 1844–1853. doi:10.1021/acs.est.7b04379
- Wang, T., Wang, J., Tang, Y., Shi, H., and Ladwig, K. (2009). Leaching characteristics of arsenic and selenium from coal fly ash: role of calcium. *Energy and Fuels* 23 (6), 2959–2966. doi:10.1021/ef900044w
- Wang, Z., and Giammar, D. E. (2015). “Metal contaminant oxidation mediated by manganese redox cycling in subsurface environment,” in *Advances in the environmental biogeochemistry of manganese oxides* (American Chemical Society), 1197, 29–50. doi:10.1021/bk-2015-1197.ch002
- World Health Organization (2022). “Guidelines for drinking-water quality: fourth edition incorporating the first and second addenda,” 38. Geneva: World Health Organization, 104–108.